Eur. Phys. J. D **4**, 89–94 (1998)

**THE EUROPEAN PHYSICAL JOURNAL D**

© EDP Sciences
Springer-Verlag 1998

# Surface coverage studies of the $Al_{13}$ icosahedron by Li using density based molecular dynamics

A.M. Vichare[a] and D.G. Kanhere[b]

Department of Physics, University of Pune, Pune 411007, India

Received: 24 October 1997 / Revised: 7 April 1998 / Accepted: 29 June 1998

**Abstract.** Density based molecular dynamics has been used to investigate the ground state structures of heterogeneous binary clusters $Al_{13}Li_n$, $n = 1$, 2, 3, 4, 10, 19, 20, 21. Some of these structures have also been investigated by full Kohn-Sham based calculations. Our earlier investigations have shown that in the Al–Li cluster, the ground state configurations are the ones where the Al atoms form a core around which the Li atoms form a "cage". In the present work, we have chosen the well-known $Al_{13}$ icosahedron as the surface over which we study the evolution of the surface coverage as the number of Li atoms increases. On the basis of the earlier work, we expect that the $Al_{13}Li_{20}$ cluster would be the most stable and indeed our simulations do yield such a novel fivefold symmetric stable structure formed out of purely metal atoms. This icosahedral substrate is also used to study the coverage of the aluminum surface by lithium atoms. For a small number of Li atoms, these studies suggest that the Li–Li dimerisation is not particularly favored.

**PACS.** 61.46.+w Clusters, nanoparticles, and nanocrystalline materials – 36.40.-c Atomic and molecular clusters

## 1 Introduction

The problem of evolution and structure of finite sized systems, *e.g.* clusters, has received a major impetus with the advent of experimental and theoretical tools for production and analysis of properties of clusters. Such investigations also offer a possibility of producing novel stable clusters. A number of investigations, both theoretical and experimental, have been carried out on clusters with few atoms as well as clusters with thousands of atoms. An understanding of the physics of clusters is expected to help bridging the gap between atomic and molecular physics and condensed matter physics.

There have been a significant number of theoretical investigations on mainly homogeneous clusters pertaining to their ground state properties, for example their geometric structure [1,2]. The interest in the physics and chemistry of clusters arises due to a number of reasons like the availability of free cluster sources, their distinct shapes and characteristic electronic properties which are different from bulk and the possibility of using them as building blocks for novel nanostructured materials *etc.* Another interesting observation has been the existence of "magic numbers" in the abundance spectra of clusters, observed in experiments on simple alkali metal clusters [3]. Clusters with 2, 8, 18, 20, 40, 58 and 92 atoms were observed to be more stable and hence more abundant. This observation has been understood on the basis of closed shell configuration within the framework of the spherical jellium model.

While a significant amount of theoretical work has been done on homogeneous clusters, relatively less has been done on heterogeneous clusters. Work in this area has been primarily on impurity studies, *e.g.* an aluminum atom in a lithium cluster, a Magnesium impurity in Sodium cluster *etc.* Studies of heterogeneous clusters are computationally taxing as a large configuration space needs to be spanned for obtaining the ground state structures. A few investigations of an impurity in metal atom clusters using *ab initio* molecular dynamics method have been reported on $Li_nAl$ [4]. The results are also available on heteroatomic clusters like alkali-metal-atom-antimony ($A_nSb_4$) clusters [5], $Na_nF_n$ [6], $Na_nK_m$ [7] and $Al_nLi_n$ [8,9] $Na_nAl$ [10] and $Na_nMg$ [11] *etc.* These early investigations reveal some interesting properties like trapping of impurity atoms, clustering tendencies and enhanced stability with doping.

In the earlier work, we have carried out detailed calculations on heterogeneous $Al_nLi_7$ ($n = 1$, 7) and $AlLi_n$ ($n = 1$, 8) [8] and $Al_nLi_n$ clusters ($n = 1 - 10$ and 13) [9] using the Density Based Molecular Dynamics (DBMD) technique to determine the ground state structures. A general clustering tendency of aluminum atoms has been observed in these systems. It appears that these stable cluster geometries are dictated by the geometry of the aluminum core and the tendency of covalent bond formation between Li–Al. Thus lithium atoms arrange themselves to maximize the Li–Al bonds with tetrahedral coordination,

[a] e-mail: amv@unipune.ernet.in
[b] e-mail: kanhere@unipune.ernet.in

wherever possible. This can be understood on the basis of the fact that amongst all the bonds the Al–Al bond is stronger than the Li–Al bond and the cluster will stabilize itself by maximizing Li–Al bonds together with Al–Al bonds. Clearly, in a finite size small cluster having large surface area this can be easily achieved by placing the lithium atom on the surface. Therefore, if all the faces of the aluminum cluster are capped, the structure should become more stable. Indeed this is borne out by our calculations so far.

These observations suggest that if the surface geometry and the relative bond strengths between the Li–Al and the Li–Li bonds affect the geometry and stability of these clusters, then the icosahedral $Al_{13}$ system should present a "substrate" over which Li atoms can form a shell. Also, the structure resulting out of a complete coverage of the $Al_{13}$ surface is expected to be the most stable. Further, the "spherical" nature of the substrate also opens up a possibility of studying how lithium covers the aluminum icosahedron, if it does so. In the present paper, we investigate this problem by using the (DBMD) technique. It may be mentioned the thirteen atom clusters of simple atoms like Na, Mg and Al have already been investigated by Röthlisberger *et al.* using *ab initio* methods [12]. It turns out that out of all these systems, $Al_{13}$ retains the icosahedral symmetry indicating very small Jahn-Teller distortions and hence is very suitable for the present investigation *via* DBMD method.

The *ab initio* molecular dynamical method, which combines density functional theory with molecular dynamics has proven to be a powerful technique for probing the ground state geometries of clusters. The standard Car-Parrinello (CP) method [13] uses the Kohn-Sham (KS) formulation [14,15] and for large systems may prove to be computationally intensive. The recent development of an orbital free approach was able to achieve an independence from the orbital based description by describing the total energy completely in terms of the electron density [16]. The method is approximate in that it uses the kinetic energy functionals based on charge density only.

The DBMD method has been demonstrated to yield correct ground states for a number of clusters with bond lengths within a few percent of the actual Kohn-Sham calculation. We have extensively tested this technique by application to various small simple metal clusters like dimers and trimers of Li, Na, Mg, Al *etc.* [4,8,9]. For example, the equilibrium bond lengths obtained by DBMD method for the dimer systems like Li–Li and Al–Al are within a few percent of the KS results. The DBMD technique also correctly predicts the ground state geometry of the $Al_{13}$ cluster to be icosahedral with bond lengths to within 3% of the KS value. We have used this density based technique in our calculations primarily for it's speed, and it's ability to sustain long stable runs, thus allowing a large configuration space to be spanned.

In the next section, we briefly describe the method and the numerical details. This is followed by a presentation and discussion of the geometries obtained by our calculations.

## 2 Method and numerical details

In this section, we present a brief description of the DBMD method, which is based on an approximate description of the kinetic energy functional and the Car-Parrinello molecular dynamics. In the spirit of the Hohnberg-Kohn formulation, the total energy of the system is written in terms of the electronic charge density only and the molecular dynamics is performed by setting up the fictitious Lagrangian. Consequently, the method scales linearly with the size of the system. All the other ingredients are the same as that used in the standard Car-Parrinello molecular dynamics, for example the use of pseudopotentials and plane wave expansion, periodically repeated large unit cells and simulated annealing strategy.

Thus the total energy of a system consisting of $N_a$ atoms and $N_e$ interacting electrons, under the influence of an external field due to the nuclear charges at coordinates $\mathbf{R}_n$ can be written as a functional of the total electronic charge density $\rho(\mathbf{r})$ as

$$E[\rho(\mathbf{r}),\{\mathbf{R}_n\}] = T[\rho(\mathbf{r})] + E_{ext}\left[\rho(\mathbf{r}),\{\mathbf{R}_n\}\right] + E_c[\rho(\mathbf{r})] + E_{xc}[\rho(\mathbf{r})] + E_{ii}\left[\{\mathbf{R}_n\}\right] \quad (1)$$

where $\rho(\mathbf{r})$ is the electronic charge density, T is the kinetic energy, $E_{ext}$ is the electron-ion interaction energy $E_c$ is the electron-electron coulomb interaction energy, $E_{xc}$ is the exchange correlation energy, and $E_{ii}$ is the ion-ion interaction energy.

It may be noted that except for the first term, all the other terms can be explicit functionals of charge density only. The first term, which represents the kinetic energy of the non-interacting electron gas can be calculated only approximately in terms of $\rho(\mathbf{r})$. One of the most used approximations is given by

$$T[\rho] = T_{TF}[\rho] + T_W[\rho] \quad (2)$$

where $T_{TF}$ is the Thomas-Fermi Kinetic energy functional and $T_W$ is the Weizsacker correction. Thus,

$$T[\rho] = \frac{3}{10}(3\pi^2)^{\frac{2}{3}}\int \rho(\mathbf{r})^{5/3}d^3r + \frac{\lambda}{8}\int \frac{\nabla\rho(\mathbf{r})\cdot\nabla\rho(\mathbf{r})d^3r}{\rho(\mathbf{r})} \quad (3)$$

where $\lambda = 1$ for the original Weizsacker value.

Extensive work has been carried out using these functionals mainly on atomic systems [17] and the following improved functional has been suggested.

$$T[\rho(\mathbf{r})] = F(N_e)T_{TF}[\rho(\mathbf{r})] + T_W[\rho(\mathbf{r})] \quad (4)$$

where $T_{TF}$ is the Thomas Fermi term, $T_W$ is the gradient correction given by Weizsacker and the factor $F(N_e)$ is

$$F(N_e) = \left(1 - \frac{2}{N_e}\right)\left(1 - \frac{A_1}{N_e^{\frac{1}{3}}} + \frac{A_2}{N_e^{\frac{2}{3}}}\right) \quad (5)$$

with optimized parameter values $A_1 = 1.314$ and $A_2 = 0.0021$ [18]. At this stage, some comments on the choice of the kinetic energy functional and it's parametrisation are in order. The motivation for proposing the functional used here and it's variations have been extensively discussed by Parr *et al.* [17]. It turns out that for the correct long range behaviour and the correct cusp conditions at the nuclei, the $T_W$ component needs to be the leading term and the first term represents the statistical estimates of the difference between the true kinetic energy and the $T_W$ term. We have used the available parameters for $F(N_e)$, which are based on the kinetic energies of atoms including the core states, while the present calculations are for valence electrons only.

Ideally, the fit should be carried out using the atomic kinetic energies of valence electrons only. However, such a fit cannot be carried out obviously because the data for the kinetic energy *versus* the number of valence electrons will be very limited. Therefore, the available parameter values have been used. It turns out that the total energies are not very sensitive to the values of the parameters used in $F(N_e)$.

This is so because about 10% change in parameter $A_2$ leads to about 10% change in the value of $F(N_e)$. Considering that the kinetic energy contribution in the total energy is about 15%, the error in the total energy is very small. Indeed, this is borne out by the fact that our DBMD results are always within 10% of the Kohn-Sham values on all the systems studied so far [8,9].

Although a better fit is welcome, the results obtained so far by the DBMD method indicate that the total energies are not very sensitive to the parametrisation of $F(N_e)$. Further more, the critical structures in the present calculations, have been re worked by full Kohn-Sham calculations.

The Car-Parrinello technique is applied to the total energy functional (1) by defining the pseudo Lagrangian as

$$L = \mu \int \dot{\rho}(\mathbf{r}) d^3r + \frac{1}{2} \sum_n M_n |\dot{\mathbf{R}}_n(t)|^2 - E\Big[\rho, \{\mathbf{R}_n\}\Big] + \Big(\Lambda \int \rho(\mathbf{r}) d^3r - N_e\Big) \qquad (6)$$

where $\Lambda$ is the Lagrangian undetermined multiplier because of the normalization condition. The resulting equations are solved with the standard Verlet technique. We have found it most convenient to vary $\tilde{\rho}(\mathbf{r}) \equiv \rho(\mathbf{r})^{1/2}$, for maintaining the constraint of positivity of the electronic charge density.

All calculations have been performed using plane wave expansion for $\tilde{\rho}$ $(\mathbf{r})$. The local part of Bachelet, Hamann and Schlüter pseudopotentials [19] and the exchange correlation potential of Ceperley-Alder as interpolated by Perdew and Zunger [20] were used. A periodically repeated unit cell of length 40 a.u. with a $64 \times 64 \times 64$ mesh and time step $\Delta$t $\sim$ 20 a.u., corresponding to about $10^{-16}$ s, was used. We have chosen to use the plane wave expansion on the entire Fourier transform mesh without any truncation yielding the energy cutoff of 95 Ry.

In the dynamics run, we were able to evolve the system for $\sim$ 30 000 time steps without explicit electron quenching. All the ground state geometries have been obtained by simulated annealing by heating the systems to about 1200 K. In addition, the ground state has also been confirmed by re-heating and cooling and by starting with a different initial configuration.

Full Kohn-Sham calculations have also been carried out on some crucial systems. A periodically repeated unit cell of length of 40 a.u. with a $64 \times 64 \times 64$ FFT mesh was used. The energy cutoff used for the plane wave expansion was about 13 a.u. requiring about 40 000 reciprocal lattice vectors. The self consistent solution to the standard Kohn-Sham equations have been achieved *via* conjugate minimization technique following [15]. The pseudopotentials used are identical to the ones used in the DBMD calculations. The CP dynamics time step was 10 a.u. It was found necessary to use dynamic occupancies for the states during the iterations. The results of these calculations are discussed in the next section.

## 3 Results and discussion

As mentioned in Section 1 the free aluminum 13 cluster is known to form a stable icosahedron in it's ground state. This nearly spherical surface can lend itself well to a study of surface coverage by lithium atoms. That lithium atoms will cover the aluminum surface is suggested by the clustering tendency of the earlier Al–Li systems. Then for the $Al_{13}Li_{20}$ one would expect a five-fold symmetric structure, with lithium atoms capping all 20 faces of icosahedral aluminum core and forming five-membered rings. It is gratifying to see this expectation realized by our simulations. A study of the capping tendency of lithium atoms was motivated by these considerations. As a "spherical" surface, the $Al_{13}$ icosahedron also presents an ideal system to study the coverage of lithium atoms on the spherical surface.

In all the figures, the aluminum atoms are shown in black and the lithium atoms in white.

Figures 2–8 show the stable ground state for $Al_{13}Li_m$, $m$ = 1, 2, 3, 4, 10, 19, 20, 21 free clusters. The binding energies per atom for these clusters are shown in Figure 1 showing $m = 20$ to be energetically more stable. In all the cases, the icosahedral structure of the aluminum core is preserved.

For a single lithium atom, there are two possible postions, (i) the bridge position, *i.e.* at the center of the Al–Al bond, and (ii) at the center of the triangle. Our calculations indicate that the most stable position to be at the center of the triangle as shown in Figure 2. Further, it is interesting to observe the motion of single lithium atom on the spherical surface upon heating. In this case, lithium traces a path midway through the Al–Al bond indicating that the potential barrier for crossing the face is lower along this path. Naively one would expect the second lithium atom to go on any one of the nearest neighbor face. However, the configuration shown in Figure 3 turns out to be lower by about 0.05 eV, when it is placed on the

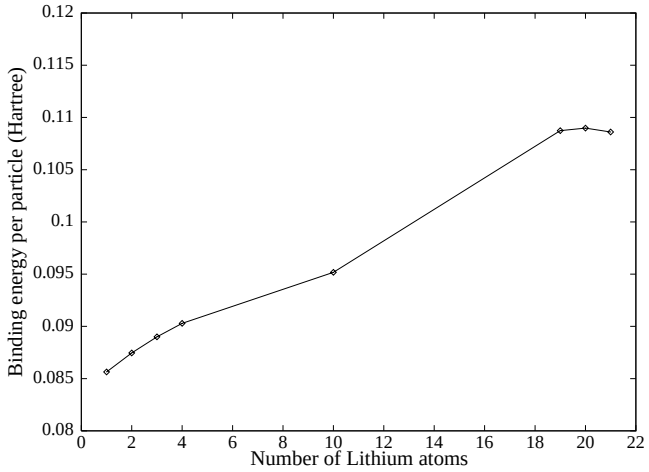


**Fig. 1.** Binding energy per atom in a.u. for the clusters investigated.

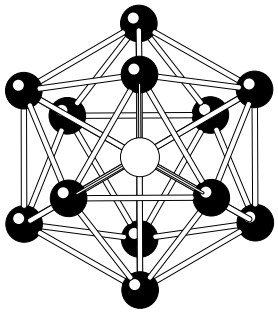

**Fig. 2.** Ground state geometry of $Al_{13}Li_1$ cluster.

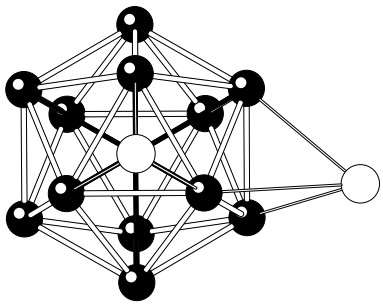

**Fig. 3.** Ground state geometry of $Al_{13}Li_2$ cluster.

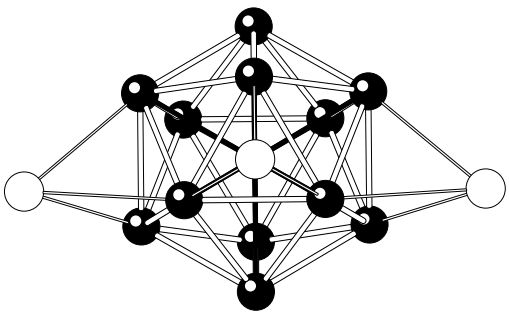

**Fig. 4.** Ground state geometry of $Al_{13}Li_3$ cluster.

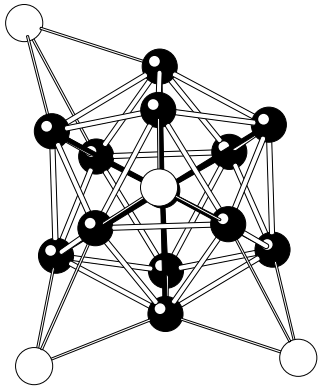

**Fig. 5.** Ground state geometry of $Al_{13}Li_4$ cluster.

**Table 1.** Bond Distances between Li–Li and Li–Al for nearest neighbor and next nearest configurations for three clusters. All distances are in a.u., *i.e.* Bohr radii.

| Cluster | Nearest | | Next Nearest | |
|---|---|---|---|---|
| | Li–Li | Li–Al | Li–Li | Li–Al |
| $Al_{13}Li_2$ | 7.00 | 5.45 | 9.81 | 5.60 |
| $Al_{13}Li_3$ | 6.91 | 5.46 | 9.77 | 5.58 |
| $Al_{13}Li_4$ | 6.54 | 5.41 | 9.72 | 5.61 |

*next* nearest neighbor site. The fact that the next nearest neighbor configurations are indeed energetically lower or at least equally probable than the nearest neighbor configurations was confirmed by separate quenching runs for $Al_{13}Li_2$, $Al_{13}Li_3$ and $Al_{13}Li_4$ systems (Figs. 3–5). This can be explained on the basis of competition between the Li–Li and Al–Li interaction energies. In an earlier work [9], it was shown that the Li–Li bond is weaker as compared to the Li–Al bond.

Table 1 lists out the smallest distances between lithium atoms and between lithium and aluminum atoms when the lithium atoms occupy nearest neighbor sites and next nearest neighbor sites. These bond lengths are larger than the Li–Li dimer bond length. Heating runs suggest the weakness of the Li–Li bond as compared to the Li–Al bond. For example, when the $Al_{13}Li_2$ system is heated, the two Li atoms were observed to traverse the icosahedral surface quite independent of each other, while being bound to the aluminum "substrate". Had the Li–Al bond been weaker than the Li–Li bond, the two lithium atoms would have dissociated first from the Al core on gradual increase in their kinetic energy, then moved together, the process finally culminating into their dissociation from each other. It was also observed that the Li atoms traverse the icosahedral surface midway through the Al–Al bonds, suggesting a lower potential barrier in comparison with the barrier presented by each Al atom. Hence, it may be concluded that the dimerisation of $Li_2$ on a spherical Al surface is not particularly favored.

The pattern continues for three and four lithium atoms and a next nearest neighbor "lattice" is seen to be favored. At half filling ($m = 10$), the picture changes and the Li

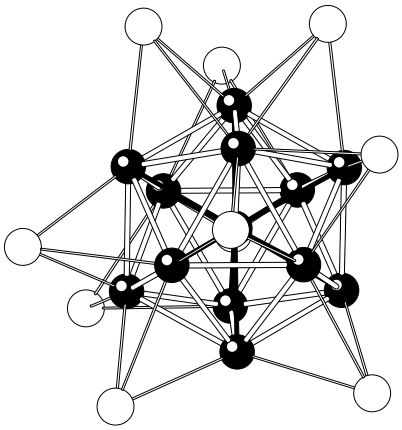

**Fig. 6.** Ground state geometry of $Al_{13}Li_{10}$ cluster.

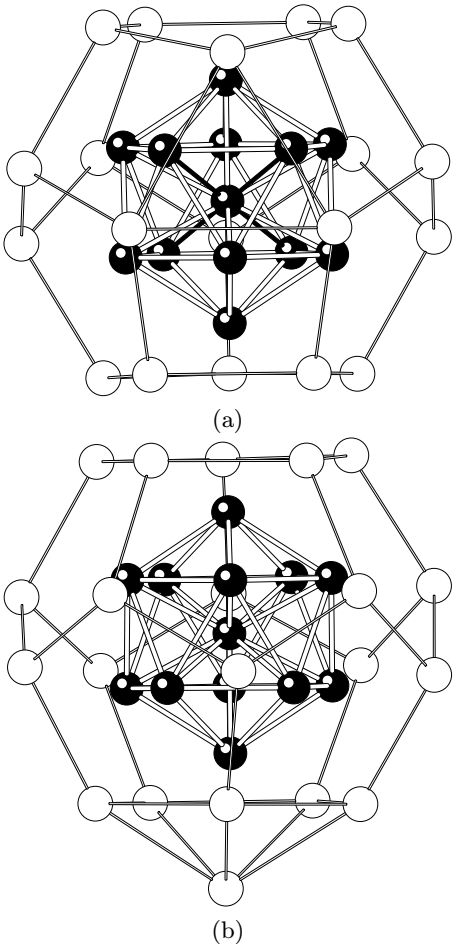

**Fig. 7.** Ground state geometries of (a) $Al_{13}Li_{19}$ and (b) $Al_{13}Li_{21}$ clusters.

atoms attempt to cover the spherical surface. One such configuration observed is shown in Figure 6. As the number of atoms go up above ten, the coverage becomes more and more complete.

A typical configuration at $m = 19$ is shown in Figure 7a. In this case, the "defect" due to lack of one lithium atom with respect to complete coverage is seen. There are six pentagonal faces, three quadrilateral faces and a triangular face. Thus the lithium atoms around the missing one adjust to maximize the bonds with the aluminum surface.

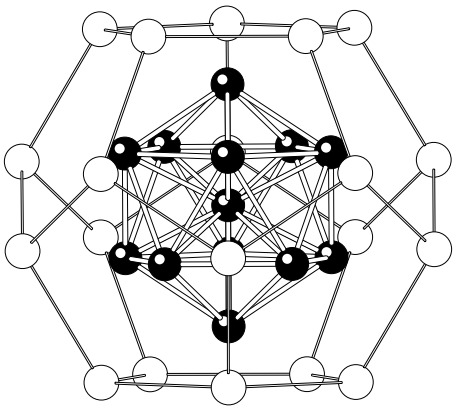

**Fig. 8.** Ground state geometry of $Al_{13}Li_{20}$ cluster.

The most interesting geometry is shown in Figure 8. This is a complete coverage of each of the faces of the aluminum core icosahedron. It is a five-fold symmetric system obtained out of purely metal atoms. It exhibits a closed lithium surface with five-membered rings. It would be interesting to see if such clusters can be experimentally realized and what would the result of an "assembly" of such clusters be.

Now we examine the geometry obtained by adding one more lithium atom to the above. This geometry is shown in Figure 7b. It is evident that the "extra" lithium atom is unable to occupy a place in the "second" geometric shell and finds a place in the "third" geometric shell, the shell with the lone Al atom at the centre being the "zeroth" shell. The radial distribution (not shown) of the atoms from the center of mass of the system, shows that the 21st lithium atom is significantly away from the "second" shell, so that it may be considered to occupy the "third" geometric shell. This also suggests that the "third" shell will be most likely completed when all the faces of the "third" shell are covered by the lithium atoms. There are 12 such faces, suggesting an fivefold symmetric third shell.

In order to verify the quality of the results of our DBMD calculations, we have also carried out full Kohn-Sham orbital based calcuations and subsequent geometry minimisations using the Car-Parinello technique for a subset of the clusters investigated using DBMD. This has been done for $Al_{13}Li_1$, $Al_{13}Li_{19}$, $Al_{13}Li_{20}$, $Al_{13}Li_{21}$ clusters. In these calculations also all the atoms, including the core Al atoms, have been allowed to move and relax. The resulting ground state equilibrium structures indicate that

1. Apart from small distortions averaging around 5%, the overall positions of all the atoms maintain the same geometry (symmetry) as the ones obtained from DBMD, suggesting small Jahn-Teller degeneracy lifts in these metallic systems.
2. The shells as seen from the center of mass have been expanded by about 5%, on an average, of their DBMD values.

**Table 2.** Comparison of total energies of the $Al_{13}Li_1$, $Al_{13}Li_{19}$, $Al_{13}Li_{20}$, $Al_{13}Li_{21}$ clusters using the DBMD technique (Col. 1) and the full Orbital Kohn-Sham calculations (Col. 2). The energies are in a.u.

| Cluster | DBMD | Kohn-Sham |
|---|---|---|
| $Al_{13}Li_{01}$ | −29.019 | −27.474 |
| $Al_{13}Li_{19}$ | −34.315 | −32.739 |
| $Al_{13}Li_{20}$ | −34.611 | −33.036 |
| $Al_{13}Li_{21}$ | −34.886 | −33.315 |

**Table 3.** Comparison of the average distances from the center of mass for each shell using the DBMD technique (Cols. 2–4) and the full orbital based Kohn-Sham technique (Cols. 5–7). All distances are in a.u.

| Cluster | DBMD | | | Kohn-Sham | | |
|---|---|---|---|---|---|---|
| | 1st shell | 2nd shell | 3rd shell | 1st shell | 2nd shell | 3rd shell |
| $Al_{13}Li_{01}$ | 4.65 | 8.54 | - | 5.09 | 8.39 | - |
| $Al_{13}Li_{19}$ | 4.75 | 8.60 | - | 5.15 | 8.99 | - |
| $Al_{13}Li_{20}$ | 4.74 | 8.63 | - | 5.35 | 9.08 | - |
| $Al_{13}Li_{21}$ | 4.74 | 8.60 | 10.03 | 5.28 | 9.09 | 10.49 |

3. The total energies for $Al_{13}Li_1$, $Al_{13}Li_{19}$, $Al_{13}Li_{20}$, $Al_{13}Li_{21}$ clusters show a near constant shift over the DBMD energies.

The relavant data namely, the average shell distances from the center of mass and the total energies are shown in Tables 2, 3. It is gratifying to see that the qualitative picture depicted by the DBMD simulations has been validated by the full Kohn-Sham calculations.

## 4 Conclusions

We have carried out density functional calculations on a system of $Al_{13}Li_m$, $m = 1, 2, 3, 4, 10, 19, 20, 21$ atoms. It is clear that in the Al–Li system, the Li atoms tend to maximize the Al–Li bonds. The coverage studies suggest that for low lithium densities the dimerisation of lithium is not particularly favored. As the number of Li atoms increase, the availability of next nearest neighbor sites reduces forcing the Li atoms to increase the Li–Al bond distances to achieve stability. Upon completion of the third geometric shell, further addition of lithium atoms starts the fourth geometric shell. These studies enable us to predict a novel stable cluster $Al_{13}Li_{20}$ having a fivefold symmetry.

Partial financial assistance from the Department of Science and Technology (DST), Government of India is gratefully acknowledged. One of us (AMV) gratefully acknowledge the research fellowships from CSIR, New Delhi. Thomas Williams and Colin Kelly are thanked for GNUplot.

## References

1. P. Jena, S.N. Khanna, B.K. Rao, *Physics and Chemistry of Finite Systems : From Clusters to Crystals*, Vol. 1 & 2 (Kluwer Academic Publ., Netherlands, 1992).
2. P. Jena, S.N. Behera, *Clusters and Nanostructured Materials* (Nova Science Publishers, Inc., New York, 1996).
3. W.D. Knight *et al.*, Phys. Rev. Lett. **52**, 2141 (1984).
4. D. Nehete, V. Shah, D.G. Kanhere, Phys. Rev. B. **53**, 2126 (1996); V. Shah, D. Nehete, D.G. Kanhere, J. Phys: Condens. Matter **6**, 10773 (1994).
5. F. Hagelberg, S. Neeser, N. Sahoo, T.P. Das, Phys. Rev. A **50**, 557 (1994).
6. J. Giraud-Girard, D. Maynau, Z. Phys. D **32**, 249 (1994).
7. A. Bol, G. Martin, J.M. Lopez, J.A. Alonso, Z. Phys. D. **28**, 311 (1993).
8. V. Shah, D.G. Kanhere, J. Phys: Condens. Matter **8**, L253 (1996).
9. V. Shah, D.G. Kanhere, C. Majumder, G.P. Das, J. Phys: Condens. Matter **9**, 2165 (1997).
10. A. Dhavale, V. Shah, D.G. Kanhere, Phys. Rev. A. (1998), in press.
11. U. Röthlisberger, W. Andreoni, Chem. Phys. Lett. **198**, 478 (1992).
12. U. Röthlisberger, W. Andreoni, P. Giannozzi, J. Chem. Phys. **96**, 1248 (1992).
13. R. Car, M. Parrinello, Phys. Rev. Lett. **55**, 685 (1985).
14. P. Hohenberg, W. Kohn, Phys. Rev. **136**, B864 (1964).
15. W. Kohn, L.J. Sham, Phys. Rev. **140**, A1133 (1965).
16. M. Pearson, E. Smargiassi, P.A. Madden, J. Phys: Condens. Matter **5**, 3221 (1993).
17. R. Parr, W. Yang, *Density Functional Theory of Atoms and Molecules* (Oxford University Press, 1989).
18. S.K. Ghosh, L.C. Balbas, J. Chem. Phys. **83**, 5778 (1985).
19. G.B. Bachelet, D.R. Hamann, M. Schluter, Phys. Rev. B. **26**, 4199 (1982).
20. J.P. Perdew, A. Zunger, Phys. Rev. B. **23**, 5048 (1981).
21. V. Shah, Ph.D thesis, University of Pune, 1997.